

## Stabilization of Protein Structure in Freeze-Dried Amorphous Organic Acid Buffer Salts

Ken-ichi IZUTSU,\*<sup>a</sup> Saori KADOYA,<sup>b</sup> Chikako YOMOTA,<sup>a</sup> Toru KAWANISHI,<sup>a</sup> Etsuo YONEMOCHI,<sup>b</sup> and Katsuhide TERADA<sup>b</sup>

<sup>a</sup>National Institute of Health Sciences; 1–18–1 Kamiyoga, Setagaya-ku, Tokyo 158–8501, Japan: and <sup>b</sup>Faculty of Pharmaceutical Sciences, Toho University; 2–2–1 Miyama, Funabashi, Chiba 274–8510, Japan.

Received May 6, 2009; accepted August 5, 2009; published online August 6, 2009

**The purpose of this study was to elucidate the physical properties and protein-stabilizing effects of some pH-adjusting excipients (carboxylic acids and their sodium salts) in frozen solutions and in freeze-dried solids. Thermal and powder X-ray diffraction (XRD) analysis indicated a high propensity of sodium citrates to form glass-state amorphous solids upon freeze-drying. Some salts (e.g., sodium succinate) crystallized in the single-solute frozen solutions. FT-IR analysis of bovine serum albumin (BSA) and bovine immunoglobulin G (IgG) in the aqueous solutions and the freeze-dried solids showed that some glass-forming salts (e.g., monosodium citrate) protected the secondary structure from lyophilization-induced perturbation. Freeze-drying of BSA at different concentrations indicated retention of the secondary structure at similar monosodium citrate/protein concentration ratios, suggesting stabilization through direct interaction that substitute water molecules inevitable for the conformation integrity. The carboxylic acid salts should provide rigid hydrogen bonds and electrostatic interactions that raise the glass transition temperature of the amorphous solids and stabilize protein structure. The relevance of the structural stabilization to the protein formulation design was discussed.**

**Key words** freeze-drying; protein formulation; stabilization; glass; Fourier transform infrared spectroscopy

The development of protein pharmaceuticals requires rational formulation design to ensure appropriate storage stability, because the degradation of such pharmaceuticals through various chemical and physical pathways not only reduces their therapeutic effects but also increases the risk of product immunogenicity.<sup>1–5</sup> Freeze-drying is a popular method of conferring long-term stability of therapeutic proteins that is not achievable in aqueous solutions. Removal of the surrounding water molecules during the freeze-drying process, however, often perturbs the protein structure, leading to irreversible aggregation in the reconstituted solutions. The structurally altered protein molecules are also prone to chemical degradation during storage.<sup>1</sup> Maintaining the protein conformation by process and ingredient (e.g., stabilizer, pH buffer, isotonic agents) optimization thus improves both the physical and chemical stability of protein formulations.

Choosing the solution pH and buffer system appropriate to a particular protein is a simple but significant element in the formulation design because the chemical and physical integrity of proteins in the aqueous solutions and freeze-dried solids depend largely on the pH.<sup>6</sup> Some buffer components also favorably or adversely affect the protein stability through direct interactions and/or through changing the local environments in the dried state. For example, freezing of certain buffer systems (e.g., sodium phosphate) often induces crystallization of a component salt and resulting shift of the local pH surrounding the proteins.<sup>7–11</sup> Freeze-drying from some buffer systems (e.g., L-histidine, citrate, or Tris) often leads to higher activity retention of proteins (e.g., coagulation factor VIII, recombinant human interleukin-1 receptor antagonist) relative to those from other buffers.<sup>12–15</sup> Conformation of the proteins lyophilized in these buffer systems is of particular interest.

Reported properties of some carboxylic acid salts, including stabilization of native protein conformation in aqueous solutions (e.g., antithrombin III)<sup>16,17</sup> and their propensity to

form glass-state amorphous solids upon lyophilization,<sup>18</sup> suggest their ability to protect protein conformation against dehydration stress through mechanisms similar to disaccharides. Non-reducing disaccharides (e.g., sucrose, trehalose) are popular stabilizers in solution and freeze-dried protein formulations. Various saccharides and polyols thermodynamically favor native protein structures over denatured states in aqueous solutions by a “preferential exclusion” mechanism.<sup>19</sup> Sucrose and trehalose protect proteins by substituting surrounding water molecules through hydrogen bonds during the freeze-drying process.<sup>4,20–22</sup> Limited molecular mobility in glass-state lyophilized disaccharide solids also protects embedded proteins from chemical degradation (e.g., deamidation) during storage.<sup>23</sup>

The present study assesses the physical properties and protein-stabilizing effects of carboxylic acid buffer systems (e.g., sodium citrate, sodium L-tartrate, sodium succinate) and their constituting salts against lyophilization-induced protein secondary structure changes. The physical properties of the frozen solutions and freeze-dried solids were studied by powder X-ray diffraction and thermal analysis. The effects of carboxylic acids and their sodium salts on the structural integrity of model proteins rich in  $\alpha$ -helices [bovine serum albumin (BSA)] or  $\beta$ -sheets [bovine immunoglobulin G (IgG)], both prior to and after the freeze-drying process, were studied by Fourier transform infrared (FT-IR) spectroscopy of the amide I band combined with a mathematical band-narrowing technique (second-derivative).<sup>24</sup> Possible mechanisms of structural stabilization and their implications for formulation design are discussed.

### Experimental

**Materials** Bovine serum albumin (A-7511, fatty acid content: approximately 0.005%, pI: 4.9), dextran 10.2k, and bovine immunoglobulin G (#64140) were purchased from Sigma-Aldrich Co. (St. Louis, MO, U.S.A.) and ICN Biomedicals Inc. (Aurora, OH, U.S.A.), respectively. Disodium hydrogen citrate sesquihydrate, monosodium citrate, and disodium(+)-tartrate dihydrate were obtained from Kanto Chemical Co. (Tokyo, Japan). Sodium

\* To whom correspondence should be addressed. e-mail: izutsu@nihs.go.jp

hydrogen L-tartrate was purchased from Alfa Aesar GmbH & Co KG (Karlruhe, Germany). Citric acid monohydrate, trisodium citrate dihydrate, sodium hydrogen L-tartrate, and other chemicals were purchased from Wako Pure Chemical, Co. (Osaka, Japan). The proteins were dialyzed overnight against buffer solutions (20 mM sodium phosphate, sodium citrate, sodium L-tartrate, sodium succinate, pH 6.0) using cellulose tubing (MWCO 14,000, Viskase Co., Darien, IL, U.S.A.). The dialyzed protein solutions were centrifuged (1500×g) and filtered (0.45 μm PVDF, Millipore, Bedford, MA, U.S.A.) before the freeze-drying study. Precipitation during dialysis reduced the IgG concentrations to 15–20 mg/ml in the resulting solutions. Monosodium succinate solution was prepared by mixing equivalent amounts of succinic acid and disodium succinate.

**Freeze-Drying** Freeze-drying was performed using a Freezone-6 lyophilizer equipped with temperature-controlled trays (Labconco, Kansas City, MO, U.S.A.). Aqueous solutions containing protein (10, 50 mg/ml) and various concentrations of excipients in flat-bottom glass vials (300 μl, 13 mm diameter) were placed on the shelf of the freeze-drier at room temperature. Some of the samples also contained low concentrations (1.5–10 mM) of the corresponding buffer system salts that were originally in the dialyzed protein stock solutions. The shelf was cooled to –40 °C at 0.5 °C/min and then maintained at this temperature for 2 h before the primary drying process. The frozen solutions were dried under vacuum (21 mTorr), with the shelf temperature maintained at –40 °C for 15 h, –30 °C for 6 h, and 35 °C for 6 h. The shelf was heated at a rate of 0.2 °C/min between the drying steps. The vials were sealed with rubber closures under vacuum. A pH meter (D-51, Horiba Ltd., Kyoto, Japan) and an electrode (9669-10D) were used to measure the pH values of solutions containing protein (e.g., BSA) and excipients. The pH values of other solutions were obtained using a pH meter (HM-60G, TOA-DKK Co., Tokyo).

**Thermal Analysis** Thermal analysis of frozen solutions and dried solids was carried out using a differential scanning calorimeter (Q-10, TA Instruments, New Castle, DE, U.S.A.) and software (Universal Analysis 2000, TA Instruments). Aliquots of aqueous solutions (10 μl) in aluminum cells were cooled from room temperature at 10 °C/min and then scanned from –70 °C at 5 °C/min. Freeze-dried solids (0.5–1 mg) in hermetic aluminum cells were subjected to thermal analysis from –30 °C at 5 °C/min under nitrogen gas flow. Maximum inflection points in the heat flow discontinuities were assigned as glass transitions of maximally freeze-concentrated phases in frozen solutions ( $T_g'$ ) and glass transitions of freeze-dried solids ( $T_g$ ).

**Powder X-Ray Diffraction (XRD) Analysis** Powder X-ray diffraction patterns were obtained at room temperature using a Rint-Altima diffractometer (Rigaku, Tokyo, Japan) with CuKα radiation at 40 kV/50 mA. The samples were scanned through the range 5° < 2θ < 35° at an angle speed of 5°/min.

**Measurement of Residual Water** The amount of water in the freeze-dried solids suspended in dehydrated methanol was determined by the Karl–Fischer method using an AQP-6 volumetric titrator (Hiranuma Sangyo, Ibaraki, Japan).

**Fourier-Transform Infrared Spectroscopy (FT-IR)** The secondary structures of proteins were analyzed using an FT-IR system (MB104 spec-

trophotometer (ABB Bomen, Quebec, Canada) with PROTA (Bomen/Vysis) and GRAMS/32 (Galactic Ind. Co.) software. Transmission spectra of freeze-dried proteins were obtained from 256 scans of pressed disks containing freeze-dried solids (approx. 1 mg protein) and potassium bromide (approx. 250 mg) at a resolution of 4 cm<sup>-1</sup>. Spectra of aqueous protein solutions (10 mg/ml) were recorded from 512 scans using an infrared cell with CaF<sub>2</sub> windows and a film spacer (6 μm). Reference spectra were recorded with the corresponding buffer and excipient solutions to obtain the absorbance spectra using an automated subtraction algorithm in PROTA. The second-derivative spectra obtained with the Savitski–Golay derivative function (7-point smoothing) were baseline-corrected and area-normalized in the amide I region (1600–1715 cm<sup>-1</sup>).<sup>25,26)</sup>

## Results

The physical properties of organic acids and their sodium salts are summarized in Table 1. Thermal analysis indicated varied propensities of the excipients to crystallize in the frozen solutions. Frozen monosodium L-tartrate solution showed two exotherm peaks that indicate eutectic crystallization. Pairs of exothermic and endothermic peaks indicated eutectic solute crystallization and subsequent melting in the frozen mono- and disodium succinate solutions. A flat thermogram in the heating scan suggested crystallization of succinic acid in the cooling process. Other frozen excipient solutions showed thermal transition of the freeze-concentrated non-ice phase at certain temperatures ( $T_g'$ : glass transitions of maximally freeze-concentrated phases).<sup>4,27)</sup> Physical properties of some frozen buffer solutions (50 mM, pH 6.0) reflected those of the constituent salts. Frozen sodium citrate and sodium L-tartrate buffer solutions showed  $T_g'$  at –41.6 and –39.7 °C, respectively. In contrast, eutectic crystallization of their constituent salts resulted in an exotherm peak (–28.8 °C) and an endotherm peak (–9.6 °C) in the frozen sodium succinate buffer. The addition of BSA (10 mg/ml) and accompanying small amount of the buffer components (1.5 mM, pH 6.0) reduced the pH variation of the aqueous excipient (50 mM) solutions. A higher transition temperature ( $T_g'$ ) and the eutectic crystallization temperatures suggested reduced mobility of solute molecules in the freeze-concentrated mixture with BSA.<sup>8)</sup>

Figure 1 shows thermograms of freeze-dried excipient solids. Heating scans of cake-structure freeze-dried monosodium L-tartrate, succinic acid, and monosodium succinate solutions

Table 1. Physical Properties of Carboxylic Acid and Their Sodium Salts

Excipients <sup>a)</sup>	Frozen solutions				Freeze-dried solids		
	w/o BSA		with 10 mg/ml BSA		with 10 mg/ml BSA		
	pH	Thermal property	pH	Thermal property	Crystallinity <sup>b)</sup>	Thermal property	Residual water (%)
Na <sub>3</sub> -citrate	8.51	$T_g'$ : –43.0 ± 1.2 °C	7.06	$T_g'$ : –35.8 ± 0.1 °C	Amorphous	$T_g$ : 74.9 ± 2.0 °C	5.2 ± 0.9
Na <sub>2</sub> H-citrate	5.28	$T_g'$ : –39.1 ± 0.0 °C	5.30	$T_g'$ : –31.6 ± 0.2 °C	Amorphous	$T_g$ : 78.2 ± 2.6 °C	5.1 ± 0.9
NaH <sub>2</sub> -citrate	3.72	$T_g'$ : –33.2 ± 0.2 °C	3.97	$T_g'$ : –24.4 ± 1.1 °C	Amorphous	$T_g$ : 61.1 ± 1.8 °C	5.2 ± 0.0
Citric acid	2.29	$T_g'$ : –55.0 ± 0.3 °C	2.63	n.d.	Amorphous	$T_g$ : 43.7 ± 1.8 °C	5.5 ± 1.8
Na <sub>2</sub> -L-tartrate	7.24	$T_g'$ : –40.0 ± 0.1 °C	6.73	$T_g'$ : –32.6 ± 0.1 °C	Amorphous	$T_g$ : 68.8 ± 2.6 °C	4.9 ± 2.1
NaH-L-tartrate	3.50	Exotherm: –26.2, –15.0 °C	3.72	Exotherm: –10.9 °C	Amorphous	$T_g$ : 56.6 ± 3.8 °C	7.0 ± 2.2
L-Tartric acid	2.26	$T_g'$ : –56.6 ± 0.8 °C	2.56	n.d.	Amorphous	$T_g$ : 43.7 ± 1.8 °C	8.4 ± 0.4
Na <sub>2</sub> -succinate	8.00	Exotherm: –36.6 °C Endotherm: –7.8 °C	6.90	Exotherm: –21.3 °C Endotherm: –8.4, –6.0 °C	Amorphous	n.d.	5.3 ± 1.1
NaH-succinate <sup>c)</sup>	4.73	Exotherm: –25.0 °C Endotherm: –8.1 °C	4.81	$T_g'$ : –39.5 ± 0.7 °C Endotherm: –7.9 °C	Amorphous	$T_g$ : 49.2 ± 3.7 °C	7.7 ± 1.2
Succinic acid	2.82	Unclear	3.41	Exotherm: –17.6 °C	Amorphous	$T_g$ : 42.0 ± 6.2 °C	6.0 ± 1.3

a) 50 mM. b) Obtained by powder X-ray diffractometry. c) Prepared by mixing and disodium succinate and succinic acid.

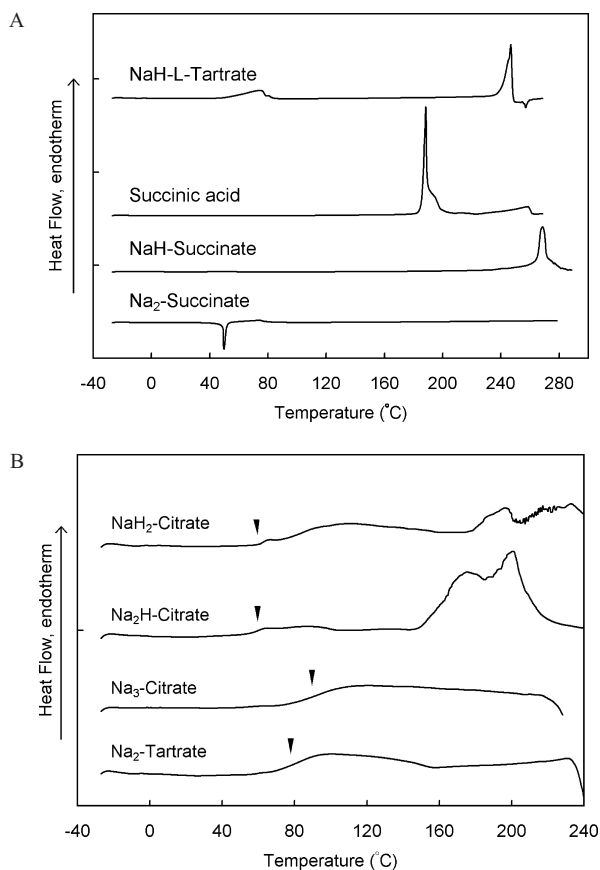


Fig. 1. Thermograms of Freeze-Dried Excipients (0.5–1 mg, 50 mM in Initial Solutions) Scanned from  $-30^{\circ}\text{C}$  at  $5^{\circ}\text{C}/\text{min}$

The solids presenting crystallization or melting peaks (A) and glass transitions (B) are shown at different heat flow scales. Arrowheads denote glass transitions of the freeze-dried solids ( $T_g$ ).

(50 mM) showed endotherm peaks that indicate melting of the crystalline moiety (Fig. 1A). A crystallization exotherm at approximately  $50^{\circ}\text{C}$  indicated the existence of an amorphous region in the freeze-dried disodium succinate solid. Frozen citric acid and L-tartaric acid solutions collapsed during the primary drying process, presumably because their  $T_g$ 's were lower than the product temperature. Some diffraction peaks in powder X-ray diffraction patterns suggested partial crystallization of succinic acid and some salts (monosodium L-tartrate, disodium succinate) lyophilized in the absence of the protein (Fig. 2, some data not shown). Other organic acid salts formed glass-state amorphous solids during freeze-drying (Fig. 1B).

Co-lyophilization of the excipients (50 mM) with BSA (10 mg/ml) resulted in cylindrical cake-structure solids. Powder X-ray diffraction (XRD) analysis of the freeze-dried solids showed halo patterns that indicate largely amorphous components (Fig. 2). Most of the freeze-dried solids showed glass transitions at temperatures close to or much higher than room temperature in the thermal analysis (Table 1). The absence of a crystal melting peak in the heating scan (e.g., monosodium citrate:  $217^{\circ}\text{C}$ ) also indicated the limited excipient crystallinity in the co-lyophilized solids. Karl-Fischer titrimetry indicated a relatively high residual water content in the freeze-dried solids (Table 1). The high protein mass ratio was one likely reason for the high residual water content in the solids freeze-dried without the organic acid salts.

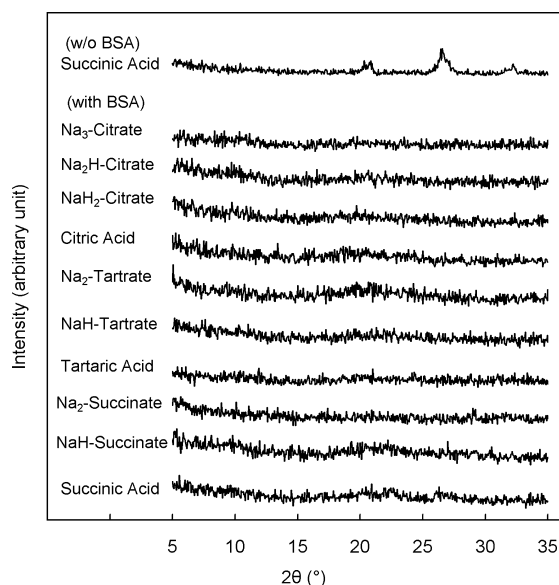


Fig. 2. Powder X-Ray Diffraction (XRD) Patterns of Excipients (50 mM) Freeze-Dried with or without BSA (10 mg/ml) and Corresponding Buffer Salts (1.5 mM)

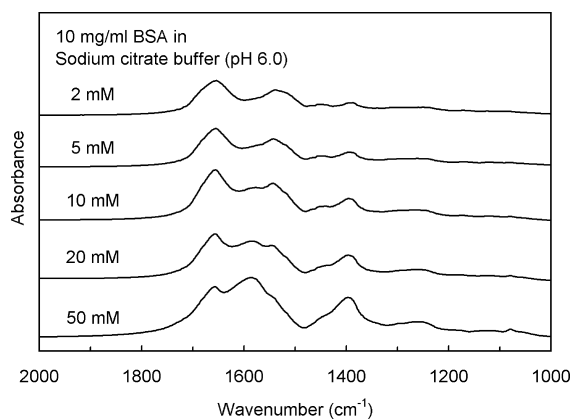


Fig. 3. FT-IR Spectra of BSA Freeze-Dried from Solutions Containing the Protein (10 mg/ml) and Various Concentrations (1.5–50 mM) of Sodium Citrate Buffer (pH 6.0)

FT-IR analysis was performed to elucidate the effect of buffer salts on the lyophilization-induced protein conformation change.<sup>2,24,25</sup> The following experiments were performed at certain (2–50 mM) buffer salt concentrations because of their overlapping absorbance in the co-lyophilized protein amide I band region ( $1600\text{--}1700\text{ cm}^{-1}$ ) (Fig. 3). Figure 4 shows area-normalized second-derivative amide I spectra of BSA in solids freeze-dried from four buffer systems (20 mM, sodium phosphate, sodium citrate, sodium L-tartrate, sodium succinate, pH 6.0). A spectrum of the protein in its initial aqueous solution (10 mg/ml, 20 mM sodium citrate buffer, pH 6.0) was also included for comparison. The protein showed practically identical spectra in the four buffer solutions studied (Fig. 5). Freeze-drying of the protein from the buffer systems resulted in a varied extent of the lyophilization-induced structural perturbation as observed in the broad amide I spectra and reduced  $\alpha$ -helix band ( $1656\text{ cm}^{-1}$ ) intensity.<sup>2,24,28–30</sup> Larger structural changes were suggested in freeze-drying of the protein from sodium phosphate and sodium succinate buffer solutions.

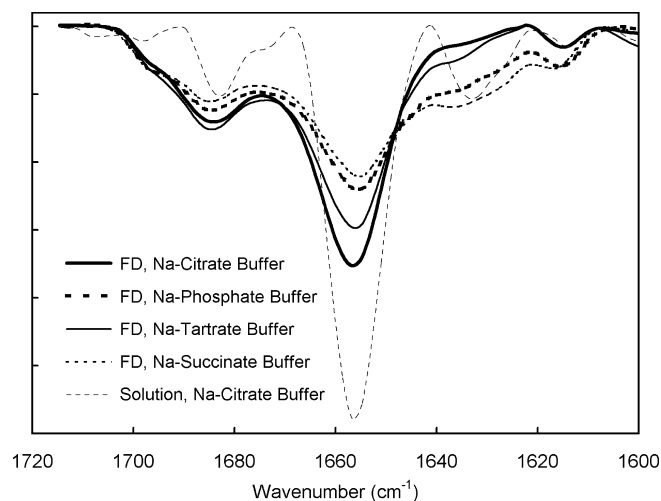


Fig. 4. Area-Normalized Second-Derivative Amide I Spectra of BSA Freeze-Dried from Solutions Containing the Protein (10 mg/ml) in Various Buffer Systems (20 mM, pH 6.0)

Fine dotted line denotes second-derivative spectra of BSA in the aqueous sodium phosphate buffer solution.

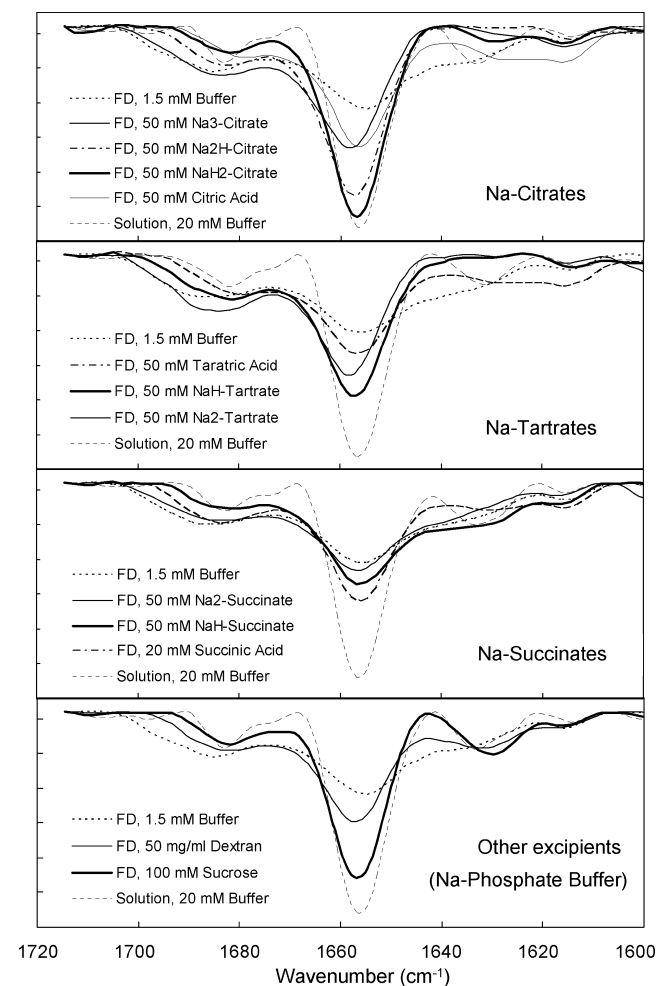


Fig. 5. Area-Normalized Second-Derivative Amide I Spectra of BSA Freeze-Dried from Aqueous Solutions Containing the Protein (10 mg/ml), Buffer Salts (1.5 mM), and Excipients (50 mM)

Fine dotted line denotes second-derivative spectra of BSA in the corresponding buffer solutions.

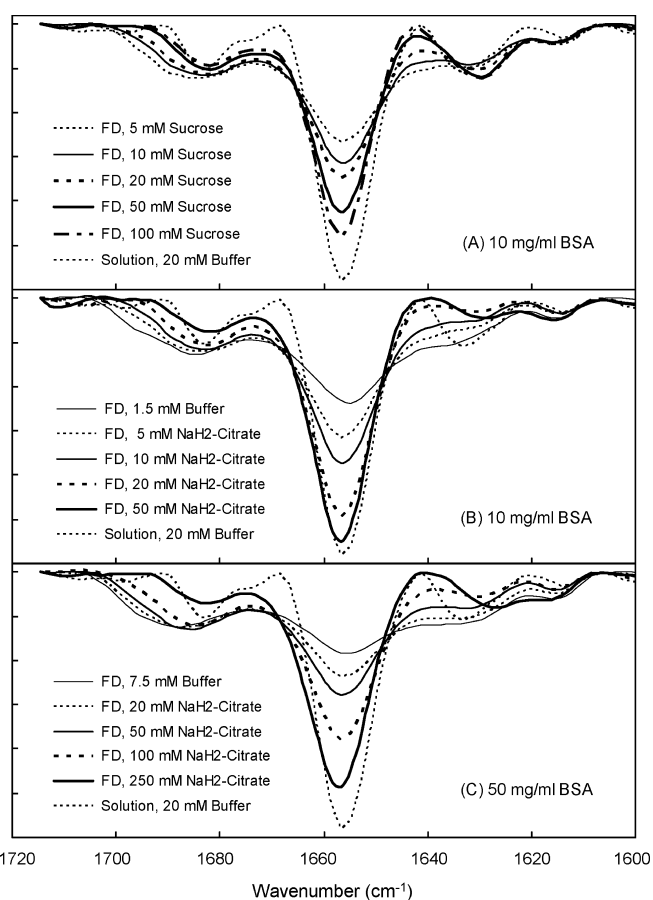


Fig. 6. Effect of Co-solutes on the Area-Normalized Second-Derivative Amide I Spectra of BSA Lyophilized at Different Concentrations (A, B: 10 mg/ml, C: 50 mg/ml).

Figure 5 shows area-normalized second-derivative amide I spectra of BSA freeze-dried with the organic acids and their salts (50 mM). Spectra of the protein in the corresponding buffer solutions (20 mM, pH 6.0) are also included. Freeze-drying of BSA (10 mg/ml) with the low concentration buffer components (1.5 mM) induced similar substantial structural changes. Monosodium citrate (50 mM) was most effective at retaining the large  $\alpha$ -helix band that characterized the native protein structure upon freeze-drying. The spectra of BSA lyophilized at different concentrations (10, 50 mg/ml, Fig. 6) suggested the structure stabilized by monosodium citrate, which effect depended roughly on the salt/protein mass ratios. The  $\alpha$ -helix band intensity reached a plateau at the salt concentrations (20–50 mM) lower than that of sucrose. Further addition of the salt induced a broader  $\alpha$ -helix band presumably because of the overlapping absorbance (data not shown).

Other salts showed varied effects on the freeze-dried protein structures (Fig. 5). Disodium citrate and monosodium L-tartrate allowed BSA to retain its secondary structure to a lesser extent upon freeze-drying, compared to monosodium citrate. Trisodium citrate and citric acid were less effective at protecting the protein structure. Other organic acids and their salts showed a limited ability to protect the native protein conformation upon freeze-drying. The effect of succinic acid was studied at a lower (20 mM) concentration because of the large overlapping absorbance in the amide I region. Insuffi-

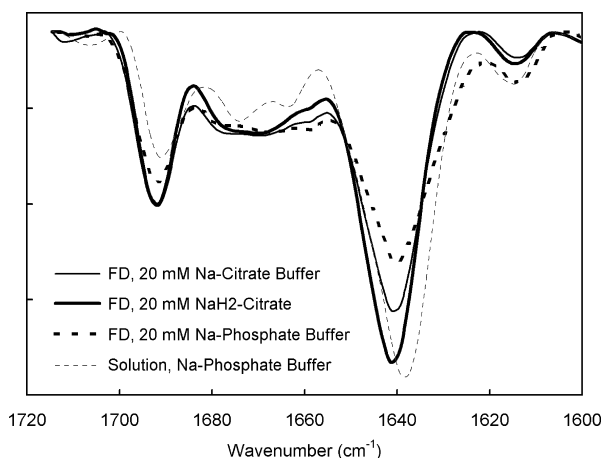


Fig. 7. Area-Normalized Second-Derivative Amide I Spectra of Immunoglobulin G in an Aqueous Buffer Solution (10 mg/ml) and Freeze-Dried Solids

The initial monosodium citrate solution (20 mM) also contained a lower (10 mM) concentration of sodium citrate buffer salts.

cient intermolecular interaction with co-lyophilized protein due to steric hindrance should explain the lower structure-stabilizing effect of dextran 10.2k compared to sucrose.<sup>31)</sup> No apparent relationship between the structure-stabilizing effect and the glass transition temperatures ( $T_g$ ) or residual water content of the freeze-dried solid (Table 1) was observed.

Second-derivative amide I spectra of bovine IgG showed predominant intramolecular ( $1637\text{ cm}^{-1}$ ) and intermolecular ( $1692\text{--}1695\text{ cm}^{-1}$ )  $\beta$ -sheet bands (Fig. 7). The reduced intramolecular  $\beta$ -sheet band intensity indicated that IgG freeze-dried from sodium phosphate buffer (20 mM, pH 6.0) had a partially altered structure. Monosodium citrate (50 mM) allowed the IgG to retain the intramolecular  $\beta$ -sheet band upon freeze-drying. Retention of the predominant bands at different wavenumbers strongly suggested the effect of salt to stabilize native protein conformation rather than an artifact induced by the overlapping absorption.

## Discussion

The results indicate that some organic acid salts form glass-state amorphous solids that protect proteins from structural change during freeze-drying. The carboxylic acids and their sodium salts showed varied physical properties in the frozen solutions and their dried solids.<sup>4)</sup> A network of rigid carboxyl/carboxylate interaction and hydrogen bonds should explain the high glass transition temperature of the lyophilized amorphous sodium citrate solids.<sup>32,33)</sup> Our previous study also showed contribution of rigid molecular interactions to form glass-state solids by co-lyophilization of citric acid and L-arginine.<sup>34)</sup> Many protein solutions have their  $T_g'$  at temperatures (approx.  $-10^\circ\text{C}$ ) higher than those of smaller molecules.<sup>27)</sup> The addition of proteins should reduce the mobility of other solute molecules in the freeze-concentrated phase, and thus prevent eutectic solute crystallization.

Freeze-drying of the protein in the sodium phosphate (20 mM) or lower concentrations of the carboxylic acid buffers (1.5 mM) perturbed their secondary structure. The structurally perturbed molecules usually return to their native structure upon re-hydration, whereas misfolding and/or binding between exposed hydrophobic regions are major causes

of the lyophilization-induced protein aggregation. The structurally altered protein molecules are also prone to chemical degradation during storage.<sup>1,2,24)</sup> Some glass-forming organic acid sodium salts (e.g., sodium citrates) maintained the native secondary structure of co-lyophilized BSA and IgG. Such structural stabilization would explain the higher residual activity of proteins after freeze-drying from certain buffer systems.<sup>12–16)</sup>

The organic acids should protect proteins through several mechanisms in the different physical states prior to and during the freeze-drying process. The fatty acid-poor BSA is most resistant to heat denaturation in weakly acidic to neutral (pH 5–7) solutions.<sup>35)</sup> Freeze-drying of the protein in the region (pH 6.0) resulted in varied secondary structures depending on the buffer systems. Observed structural stabilization at certain salt/protein concentration ratios indicated the contribution of the direct interactions. It is highly plausible that the effective buffer salts provide proteins hydrogen bonds that substitute for those of the surrounding water molecules inevitable to retain the conformation. In addition, the lower effective concentration of monosodium citrate compared to sucrose suggested the contribution of electrostatic (ion–ion, ion–dipole) interactions between the salt anion (hydroxycarboxylate ion) and basic amino acid residues on protein surfaces for the structural stabilization.<sup>17,36,37)</sup> The high  $T_g$  of the dried solids indicated mixing of the protein and salts required for the interaction. The topic of protein-stabilizing molecular interactions in the dried states, including the effect of differently ionized functional groups, will require further study for elucidation. The limited mobility of the surrounding molecules should prevent chemical degradation of the protein in glass-state solids. Similar structural (thermodynamic) and chemical (kinetic) stabilization of embedded proteins has been reported in disaccharides.<sup>22,23)</sup> Some of the buffer components should also protect proteins from cold denaturation in the aqueous solutions and in the frozen solutions. The citrate<sup>3-</sup> and L-tartrate<sup>2-</sup> ions are ‘kosmotropic’ anions that thermodynamically stabilize native protein structures by being preferentially excluded from the immediate surface of the protein molecules.<sup>16,17,22,38–41)</sup> In other words, the proteins are preferentially hydrated in the solute solutions.

The difference in the structure and physical properties would explain the varied protein-stabilizing effect of the organic acid salts through the above-mentioned mechanisms. Solution pH and anion structure are major factors that determine the thermal stability of proteins in aqueous carboxylic acid salt solutions.<sup>17)</sup> Some di- and tricarboxylic acid salts protect proteins from thermal denaturation. The number of carboxyl and hydroxyl groups should be also likely to be important in protecting the secondary structure of BSA through the water-substituting hydrogen bonds and electrostatic interactions against the dehydration stress. The limited structure-stabilizing effect of succinic acid and its salts during freeze-drying, in spite of their apparent effect to improve the thermal stability of proteins in aqueous solutions, suggests that the hydroxyl group makes a large contribution to the structural stabilization against dehydration stresses. Possible salt crystallization at a higher salt/protein concentration ratio should further reduce the stabilizing interactions between them. Monosodium citrate should satisfy various requirements (e.g., sufficient functional groups, appropriate ionized

states, propensity to form glass-state amorphous solids) for protein-stabilizing interactions in the dried states.

Our results emphasize the importance of choosing an appropriate buffer system when developing freeze-dried protein formulations. Salts that have a higher propensity for crystallization should be avoided especially at lower excipient/protein concentration ratios. Significant stabilizing effects of some organic acid salts are applicable to the design of sugar-free formulations. Some buffer components also raise the glass transition temperature of co-lyophilized disaccharide solids.<sup>42,43</sup> The retention of protein structural integrity in the amorphous salt solids would also be relevant to other applications of proteins in ionic environments, including enzyme reactions in ionic liquids (RTMS: room temperature molten salts).<sup>44–46</sup> Careful optimization of ingredients based on the physical and chemical properties of the excipients should ensure the optimal processing and storage stability of protein formulations.

**Acknowledgements** This work was supported in part by the Japan Health Sciences Foundation (KHB1006).

#### References

- Chang B. S., Beauvais R. M., Dong A., Carpenter J. F., *Arch. Biochem. Biophys.*, **331**, 249–258 (1996).
- Prestrelski S. J., Tedeschi N., Arakawa T., Carpenter J. F., *Biophys. J.*, **65**, 661–671 (1993).
- Hermeling S., Crommelin D. J., Schellekens H., Jiskoot W., *Pharm. Res.*, **21**, 897–903 (2004).
- Shalaev E. Y., Johnson-Elton T. D., Chang L., Pikal M. J., *Pharm. Res.*, **19**, 195–201 (2002).
- MacKenzie A. P., *Bull. Parenter. Drug Assoc.*, **20**, 101–130 (1966).
- Akers M. J., Vasudevan V., Stickelmeyer M., *Pharm. Biotechnol.*, **14**, 47–127 (2002).
- Williams-Smith D. L., Bray R. C., Barber M. J., Tsopanakis A. D., Vincent S. P., *Biochem. J.*, **167**, 593–600 (1977).
- Murase N., Franks F., *Biophys. Chem.*, **34**, 293–300 (1989).
- Sarciaux J. M., Mansour S., Hageman M. J., Nail S. L., *J. Pharm. Sci.*, **88**, 1354–1361 (1999).
- Pikal-Cleland K. A., Rodriguez-Hornedo N., Amidon G. L., Carpenter J. F., *Arch. Biochem. Biophys.*, **384**, 398–406 (2000).
- van den Berg L., Rose D., *Arch. Biochem. Biophys.*, **81**, 319–329 (1959).
- Hynes H. E., Owen C. A. J., Bowie E. J., Thompson J. H. J., *Blood*, **34**, 601–609 (1969).
- Osterberg T., Fatouros A., Mikaelsson M., *Pharm. Res.*, **14**, 892–898 (1997).
- Chang B. S., Reeder G., Carpenter J. F., *Pharm. Res.*, **13**, 243–249 (1996).
- Labrude P., Vigneron C., *J. Pharm. Pharmacol.*, **32**, 305–307 (1980).
- Busby T. F., Atha D. H., Ingham K. C., *J. Biol. Chem.*, **256**, 12140–12147 (1981).
- Kaushik J. K., Bhat R., *Protein Sci.*, **8**, 222–233 (1999).
- Li J., Chatterjee K., Medek A., Shalaev E., Zografi G., *J. Pharm. Sci.*, **93**, 697–712 (2004).
- Arakawa T., Timasheff S. N., *Biochemistry*, **21**, 6536–6544 (1982).
- Carpenter J. F., Crowe J. H., *Biochemistry*, **28**, 3916–3922 (1989).
- Izutsu K., Yoshioka S., Terao T., *Pharm. Res.*, **10**, 1232–1237 (1993).
- Carpenter J. F., Prestrelski S. J., Arakawa T., *Arch. Biochem. Biophys.*, **303**, 456–464 (1993).
- Franks F., *Dev. Biol. Stand.*, **74**, 9–18 (1992).
- Dong A., Prestrelski S. J., Allison S. D., Carpenter J. F., *J. Pharm. Sci.*, **84**, 415–424 (1995).
- Susi H., Byler D. M., *Biochem. Biophys. Res. Commun.*, **115**, 391–397 (1983).
- Kendrick B. S., Dong A., Allison S. D., Manning M. C., Carpenter J. F., *J. Pharm. Sci.*, **85**, 155–158 (1996).
- Chang B. S., Randall C., *Cryobiology*, **29**, 632–656 (1992).
- Carter D. C., Ho J. X., *Adv. Protein Chem.*, **45**, 153–203 (1994).
- Murayama K., Tomida M., *Biochemistry*, **43**, 11526–11532 (2004).
- Luthra S., Kalonia D. S., Pikal M. J., *J. Pharm. Sci.*, **96**, 2910–2921 (2007).
- Kreilgaard L., Frokjaer S., Flink J. M., Randolph T. W., Carpenter J. F., *J. Pharm. Sci.*, **88**, 281–290 (1999).
- Kadoya S., Izutsu K., Yonemochi E., Terada K., Yomota C., Kawanishi T., *Chem. Pharm. Bull.*, **56**, 821–826 (2008).
- Inabe T., *J. Mater. Chem.*, **15**, 1317–1328 (2005).
- Izutsu K., Kadoya S., Yomota C., Kawanishi T., Yonemochi E., Terada K., *Chem. Pharm. Bull.*, **57**, 43–48 (2009).
- Gumpen S., Hegg P. O., Martens H., *Biochim. Biophys. Acta*, **574**, 189–196 (1979).
- Tian F., Middaugh C. R., Offerdahl T., Munson E., Sane S., Rytting J. H., *Int. J. Pharm.*, **335**, 20–31 (2007).
- Izutsu K., Fujimaki Y., Kuwabara A., Aoyagi N., *Int. J. Pharm.*, **301**, 161–169 (2005).
- Arakawa T., Timasheff S., *Biochemistry*, **23**, 5912–5923 (1984).
- Hofmeister F., *Arch. Exp. Pathol. Pharmacol.* (Leipzig), **24**, 247–260 (1888).
- Jensen W. A., Armstrong J. M., Giorgio J. D., Hearn M. T., *Biochim. Biophys. Acta*, **1296**, 23–34 (1996).
- Ru M. T., Hirokane S. Y., Lo A. S., Dordick J. S., Reimer J. A., Clark D. S., *J. Am. Chem. Soc.*, **122**, 1565–1571 (2000).
- Ohtake S., Schebor C., Palecek S. P., de Pablo J. J., *Pharm. Res.*, **21**, 1615–1621 (2004).
- Kets E. P., IJpelaar P. J., Hoekstra F. A., Vromans H., *Cryobiology*, **48**, 46–54 (2004).
- Fujita K., MacFarlane D. R., Forsyth M., *Chem. Commun. (Camb.)*, **2005**, 4804–4806 (2005).
- van Rantwijk F., Madeira L. R., Sheldon R. A., *Trends Biotechnol.*, **21**, 131–138 (2003).
- Ohno H., *Bull. Chem. Soc. Jpn.*, **79**, 1665–1680 (2006).